Performance comparison with different methods for ethanol/O2 biofuel cell based on NAD+ cofactor immobilized and activated by two types of carbon nanoparticles

Djamel Selloum, Vincent Techer, Abdellah Henni, Sophie Tingry, Marc Cretin, Christophe Innocent

Performance comparison with different methods for Ethanol/O_2 biofuel cell based on NAD^+ cofactor immobilized and activated by two type of carbon nanoparticles

Djamel Selloum[1*], Vincent Techer[2], Abdellah Henni[1], Sophie Tingry[2], Marc Cretin[2], Christophe Innocent[2]

[1]*Lab. Dynamic Interactions and Reactivity of Systems, Kasdi Merbah University, Ouargla, 30000, Algeria*

[2]*Institut Européen des Membranes, UMR 5635, ENSCM-UMII-CNRS, place Eugène Bataillon, 34095 Montpellier, France.*

*** Corresponding author**e-mail: selloumdjamel@gmail.com, selloum.djamel@univ-ouargla.dz (Djamel Selloum)

Abstract

Biofuel cells are an attractive alternative to conventional fuel cells, because they use biological catalysts. We report in this article the construction of an ethanol / O_2 enzymatic biofuel cell. In the first time, the performance comparison with different methods for Ethanol/O_2 biofuel cell has been study. Alcohol dehydrogenase, a Nicotinamide Adenine Dinucleotide (NAD) dependant enzyme, is immobilized with NAD^+, diaphorase and vitamin K3 (VK3) on the electrode. The oxygen is reduced at the cathode with laccase and 2,2'-azinobis(3-ethylbenzothiazoline-6-sulfonate) (ABTS).The performances of the electrodes are improved thanks to addition of carbon powder (KS6 and Super P® carbon). The benefit of the carbon particles with higher surface porosity was explained by the high porous structure that offered a closer proximity to the reactive species and improved diffusion of ethanol and oxygen within the enzyme films. Efficiency of immobilization of NAD^+ cofactor has been also demonstrated. We have shown the effect of multienzymatic reaction at the anode on the storage and operational stability. A high open circuit potential has been recorded 1.02V, demonstrating the benefit of NAD^+ immobilization with maximal power density of 300 $\mu W.cm^{-2}$. Chronoamperometric measurements show a current density of 90 $\mu A.cm^{-2}$ during 20 hours demonstrating the operational stability of the ethanol biofuel cell based on NAD^+ cofactor immobilization.

Keywords: bioelectrochemistry; enzymatic biofuel cell; carbon particles; alcohol dehydrogenase; diaphorase.

1. Introduction

The significantly environmental impact in the use of unrecoverable energy source will shortly force us to found a substitute way of energy production [1]. Fuel cells usually generate electricity through electrochemical conversion of fuels directly into electricity [2]. Biofuel cells use biocatalysts as enzymes, in regards to biological cells, to convert chemical energy into electrical energy with a low power source at room temperature and under physiological conditions. The advantage of enzymatic biofuel cells is to exploit the selectivity of enzymes and total biodegradability of the catalysts.

Biofuel cells are an attractive alternative to conventional fuel cells, because they use biological catalysts which eliminate the dependence on precious metal catalysts. Biofuel cells reported in the literature since the 1960's [3, 4].

Enzymatic biofuel cells employ enzymes to catalyze chemical reactions, thereby replacing traditional electrocatalysts [5]. These systems generate electricity under mild conditions through the oxidation of renewable energy sources [6]. The advantages of biocatalysts are reactant selectivity, activity in physiological conditions, and manufacturability. However, biofuel cells show relatively low power densities and limited stability associated with the lifetime of the enzymes. The most studied biofuel cell operates with glucose as fuel and oxygen as oxidant [7–13], in the presence of redox mediators to achieve efficient catalyst utilization.

Enzymatic biofuel cell systems offer main advantage to traditional fuel cells. Enzyme catalysts allow for a wide a variety of fuels to be utilized, because enzymes typically do not react with or get passivated by impurities in the fuel [14].

Researchers have been attempting to develop direct ethanol fuel cells (DEFCs), but there have been problems because traditional precious metal catalysts (Pt-based catalysts) are unable to efficiently catalyze the oxidation ethanol and maintain an electrode with minimal fouling at low temperatures. However, living organisms are capable of efficiently catalyzing the oxidation of

ethanol. Living organisms, such as *Pseudomonas aeruginosa*[15], acetobacter [16], and gluconobacter[17], contain enzymes that can oxidize a variety of alcohols, including ethanol. An oxidized nicotinamide adenine dinucleotide (NAD^+)-dependent dehydrogenase, such as alcohol dehydrogenase, has commonly been utilized in an enzymatic anode in biofuel cells[18]. Such enzymes oxidize the corresponding fuels with the accompanying reduction of cofactor NAD^+ to nicotinamide adenine dinucleotide (NADH). In order to collect electricity and recover NAD^+ for a continuous reaction, the enzymatically produced NADH needs to be oxidized at the supporting electrode. Since the oxidation of NADH requires a large overvoltage on a conventional electrode, typically diaphorase (an enzyme for NADH oxidation) [19, 20].

This paper describes the development of an ethanol biofuel cell based on NAD^+ cofactor immobilized and activated by two types of carbon nanoparticles. In particular, the work focused on the influence of carbon nanoparticles type on the electron transfer in attempt to improve efficiency of the bio-electrocatalytic process and in the first time, the performances of the devices were evaluated using two different methods.

2. Experimental Section

2.1. Materials

Laccase from *Trametes Versicolor* (20 U mg^{-1} solid), Diaphorase 3-20 U mg^{-1}, Alcohol Dehydrogenase 300 U mg^{-1}, β-nicotinamide adenine dinucleotide sodium salt (NAD^+), 2-methyl-1,4-naphthoquinone (VK3), Aceton, polyethylenimine (PEI), 2,2'-azinobis(3-ethylbenzothiazoline-6-sulfonate) diammonium salt (ABTS), Nafion® solution (5wt%), sodium phosphate dibasic dihydrate ($Na_2HPO_4.2H_2O$) and sodium phosphate monobasic monohydrate ($NaH_2PO_4.H_2O$) were purchased from Sigma-Aldrich and used without further purification. The phosphate buffer was prepared with $Na_2HPO_4.2H_2O$ and $NaH_2PO_4.H_2O$ pH

5, 7 or pH 9, 0.1 M. The carbon nanoparticles powder as Super P® and KS6 were purchased from TIMCAL.

2.2. Bioelectrodes preparation

The biocathode to be employed in the electroreduction of oxygen was prepared by adsorption of enzymes and mediators on the surface of the electrodes by drop casting. 333 µL of laccase 15 mg mL^{-1} and Super P® 15 mg mL^{-1} in phosphate buffer 0.1 M (pH 5) solution was mixed on a vortex mixer. Sequentially, 100 µL of the solution was mixed with ABTS 5.4 mg mL^{-1} and 10 µL Nafion®. Then, 6 µL of the preparation was coated onto Au electrode and left to dry at room temperature before keeping in a low humidity environment.

The bioanode to be employed in the oxidation of ethanol was prepared by adsorption of successive coatings separated by a dried step at room temperature. 167 µL of ADH 30 mg mL^{-1} and KS6 15 mg mL^{-1} in phosphate buffer 0.1 M (pH 7) solution was mixed on a vortex mixer and 6 µL of the preparation was pipetted onto the electrode and dried at room temperature. The same procedure was conducted for the immobilization of NAD^+ 30 mg mL^{-1} and then diaphorase 20 mg mL^{-1}. The last coating on the electrode consisted in pipetting 10 µL of VK3 60 mg mL^{-1}, 190 µL acetone and 10 µL PEI, followed by drying.

2.3. Physical characterization

Carbon powders were analyzed by scanning electron microscopy (SEM, S-4800, Hitachi), and X-Ray diffraction (PANAlyticalXpertPRO diffractometer equipped with a X'celerator detector using Ni-filtered Cu-radiation). Raman spectra were acquired using a Raman microspectrometer (Jobin-Yvon S.A.S., Horiba, France) equipped with an optical microscope under ambient conditions with a 647.1 nm laser and the acquisition range was 1000–2000 cm^{-1}.

2.4. Electrochemical measurements

The bioelectrodes were characterized separately by polarization curves performed in dioxygen-saturated phosphate buffer pH 5 0.1 M for the biocathode, or in phosphate solution pH 9, 0.1 M with 160 µL ethanol for the bioanode, after stabilization of the open circuit potential. Electrochemical measurements were performed on a potentiostat Autolab (Eco chemie, Netherlands) at 25°C in phosphate buffer, with a conventional three-electrodes system composed of a stainless-steel auxiliary electrode, a calomel saturated reference electrode and the electrode material as working electrode.

The BFC was characterized by the same electrochemical equipment. The cathode was connected to the working electrode, and the counter and reference electrodes were both connected to the anode. The catholyte solution consisted of phosphate buffer solution 0.1 M (pH 5) saturated with O_2. The anolyte solution contained ethanol 160 µL in phosphate buffer 0.1 M (pH 9). Both solutions are separated by ion exchange membrane (Nafion from Dupont USA) [21]

The open circuit potential (V_{oc}) was measured when no current flows. An equilibration time was maintained during 5min before data collection to reach maximum open circuit potential. Polarization curves, known as I-V curves, were obtained by measuring the current while slowly varying the potential between the V_{oc} and 0 V, or by applying external resistances from 100 Ω to 1 MΩ and measuring the resulting current and voltage. Current and power densities were determined using the geometric area of the electrodes.

3. Results and Discussion

3.1. Influence of carbon powder.

At first the carbon KS6 and Super P® were characterized by SEM microscopy (Fig.1A and 1B). KS6 has a sheet structure composed of particle size dimensions of the order of 1 µm and by an intense X-ray diffraction peak at 2θ=26° typical of graphitic carbon [22] (Fig. 1C). At contrary, the carbon Super P® presents a porous structure composed of smaller nanoparticules of ten nanometers (Fig. 1B) and no characteristic peak on the XRD diffraction pattern (Fig. 1C). Their impact has been studied on the electrochemical behavior of the bioelectrodes based on immobilization of laccase as cathode and diaphorase (DI) and alcohol deshydrogenase (ADH) as anode.

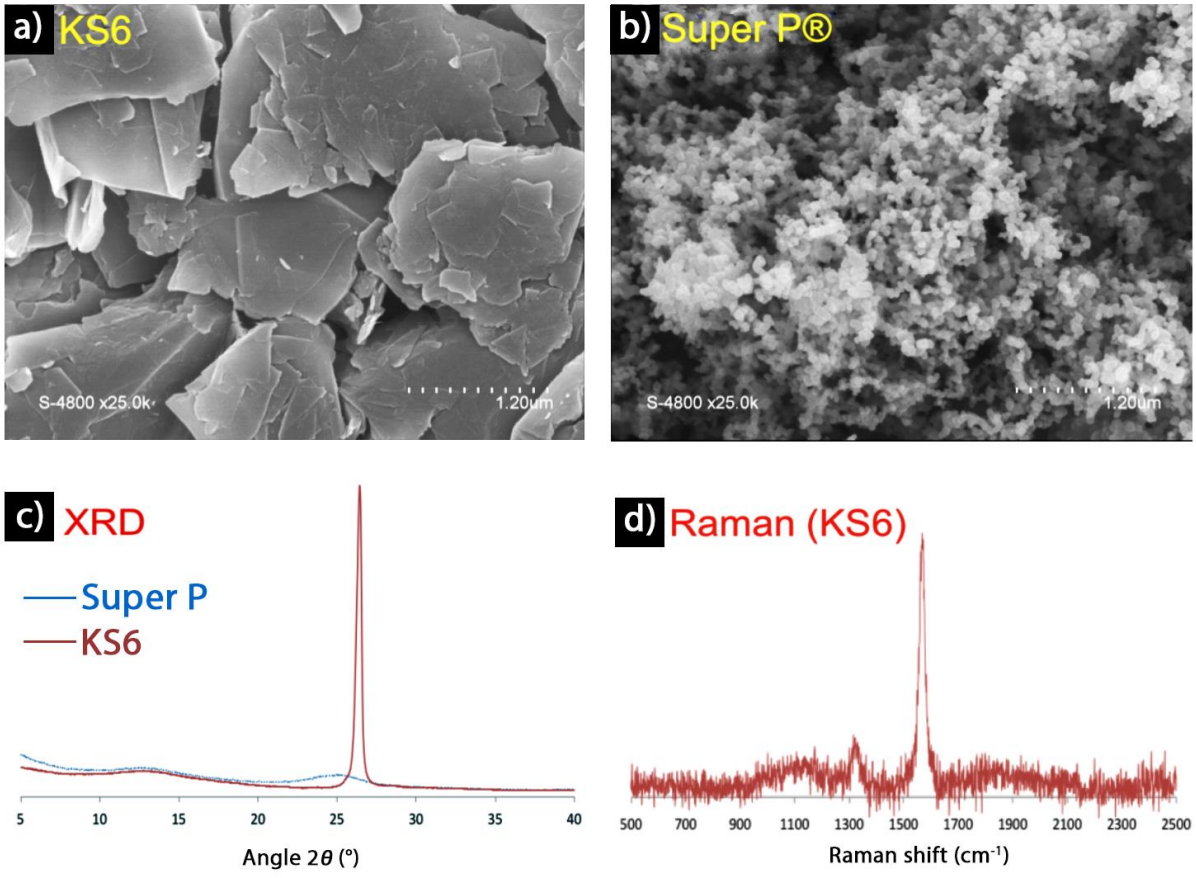

Figure 1.SEM images of carbon powders KS6 (A) and Super P® (B), scale bar is 1.2 µm. XRD spectra of the two carbons (C) and Raman spectra of KS6 (D).

The Raman spectrum of KS6 carbon powder presented in Figure 1.D displays a peak at 1582 cm^{-1}, which correspond to the crystal graphite [23].This result is in agreement with the data provided by the supplier (TIMCAL).

3.2. Characterization of bioanode.

The working of bioanode based on alcohol deshydrogenase and diaphorase immobilization is presented in figure 2. Ethanol is oxidized to aldehyde by ADH and its cofactor NAD^+. The regeneration of the cofactor is well achieved using an additional redox protein diaphorase which operates efficiently in the presence of the mediator VK3 [24].

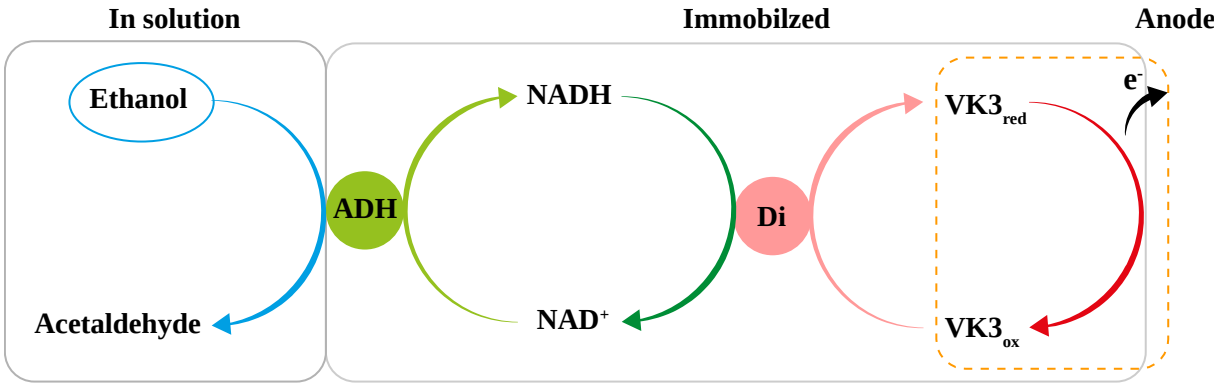

Figure 2. Schematic representation of the bioanode system.

The electrochemical behavior of the bioanode has been studied in the presence of the different carbon black powders. Fig.3 shows the catalytic activity of the bioanode in phosphate buffer solution pH 9 in the presence of ethanol.

The bioanodes exhibit activity for ethanol oxidation with a V_{oc} around -0.32 V/SCE and –0.30 V/ECS for KS6 and Super P respectively. (Fig.3).

However, in the presence of Super P®, a sharp increase of the current density and an oxidation peak at -0.15 V/ECS are observed, corresponding to the oxidation of the mediator VK3 on the electrode and also the oxidation of ethanol in the solution (see fig 2). In absence of substrate (ethanol) the value of current is very low, demonstrating the effect of ethanol oxidized by enzymatic reaction.

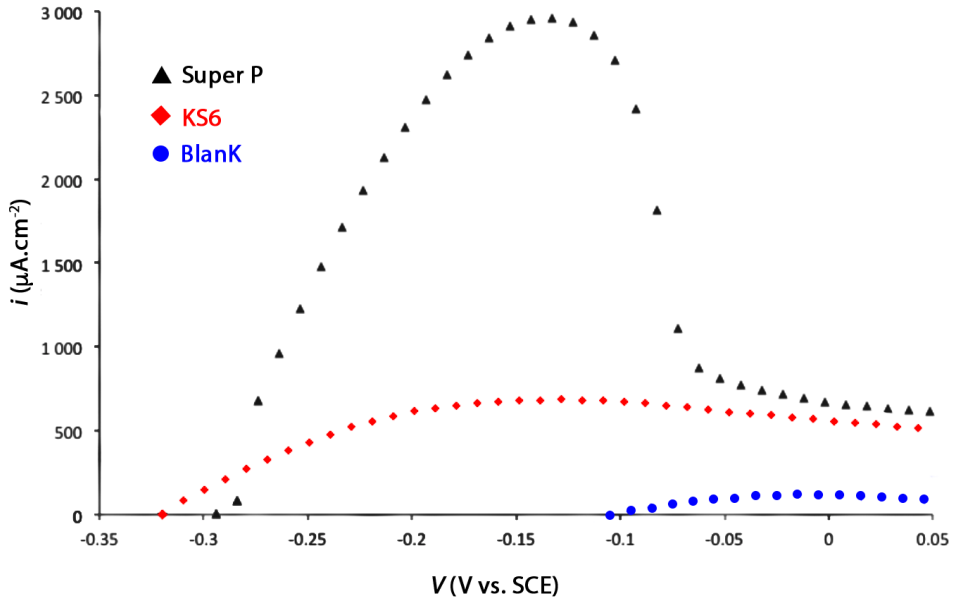

Figure 3. Polarization curve (first scan) of an ADH/NAD^+/Di/VK_3 modified electrode in phosphate buffer solution (pH 9, 0.1 M) with 70 mM ethanol and without ethanol (Blank). Comparison between carbon powders KS6 and Super P®. Scan rate 3.33 mV s^{-1}.

The high value of the peak is due to the large amount of VK3 reduced at the electrode when the substrate reacts with enzymatic chain. A decrease of the signal is observed during the second scan. The resulting values after stabilization gave the same results for electrode with Super P and KS6. Thus, electrodes with KS6 have been chosen for the elaboration of bioanode.

A poor stability has been observed by voltamperometric characterization with a loss of 31% in current density after 3 scans (Table 1).

Table 1. Stability of a KS6 modified bioanode

KS6 anode			
	V^0 (mV)	***i*** **(μA.cm^{-2}) -0.2 V**	**Current density lost**
1st scan	-415	680	-
2st scan	-420	614	-10%
3st scan	-411	470	-31%
Day+1	-198	06	-90%

A decrease of 90% of current has been observed after one day of storage at 4°C. These weak performances can be explained by the denaturation of enzyme and the loss of mediator (particularly loss of NAD^+) in the solution. On the other hand, the enzymatic cascade with alcohol deshydrogenase and diaphorase and their mediators generates a local pH modification when the VK3 is not oxidized at the electrode (open circuit).

However, the chronoamperometric characterization presented in figure 4 showed stabilization of current after 1500 s. This result demonstrates the efficiency in operational conditions of the enzymatic catalysis on the electrode. At first a decrease of current is recorded followed by a steady state which corresponds to the stationary operation of the bioanode.

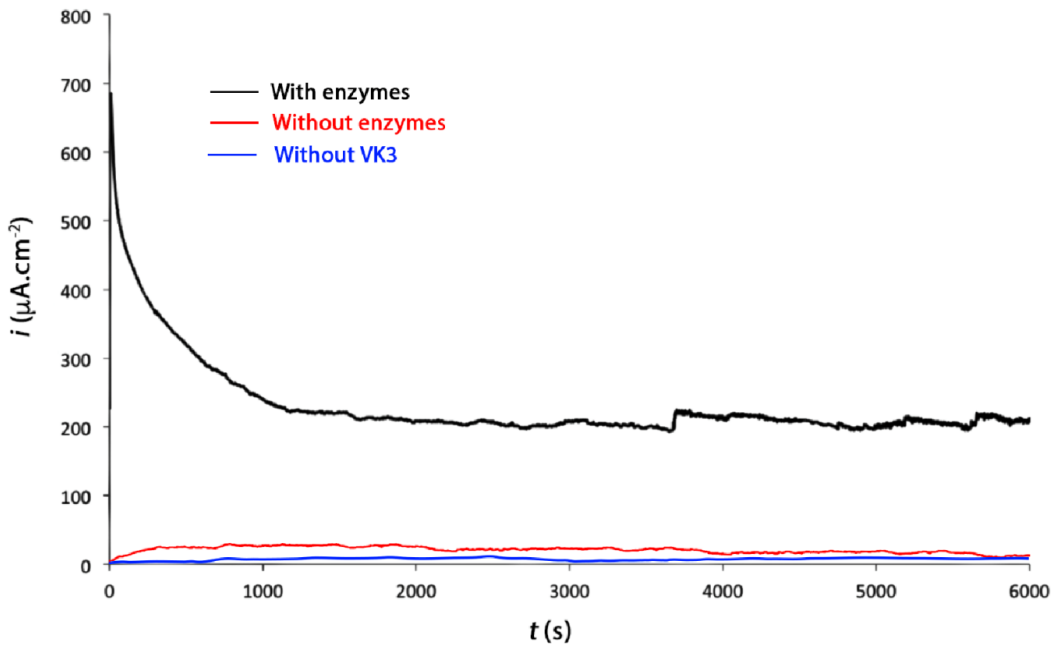

Figure 4. Chronoamperometric response at -0.2 V/SCE for a bioanode with carbon KS6 in phosphate buffer (pH 9, 0.1 M) with ethanol 70 mM, with (black curve), without enzyme (red curve) and without VK3 (blue curve).

Without enzyme no current is observed and also without VK3 (see fig 4). The presence of enzyme and VK3 is necessary to activate the catalytic cycle of enzymatic reaction according to the scheme presented in figure 2.

According to these results we can conclude that bioanode is able to work in the operating condition but a large denaturation is observed in the storage condition. This result can be explained by the reaction association on the electrode. When no potential is applied, or no connection with another electrode (cathode in the case of biofuel cell) substrate residues unremoved by rinsing, can react with enzyme at the electrode and activate the catalytic chain until the formation of reduced vitamin K3. In this condition, a high local concentration of reduced vitamin K3 occurs on the electrode. Moreover, when the catalytic chain stops by lack of substrate, the ratio of reduced and oxidized compound in the film and the variation of local

pH can affect the enzymes integrity. Accordingly the storage stability is very poor for this kind of the electrode.

To keep the integrity of the electrode, operating is necessary to evacuate electron produced by the enzymatic reactions.

3.3. Characterization of biocathode

The cathode based on immobilization of ABTS and laccase has been studied in the same way. The electrochemical reactions are depicted in figure 5. Reduction of oxygen is catalyzed by enzyme laccase and ABTS as mediator.

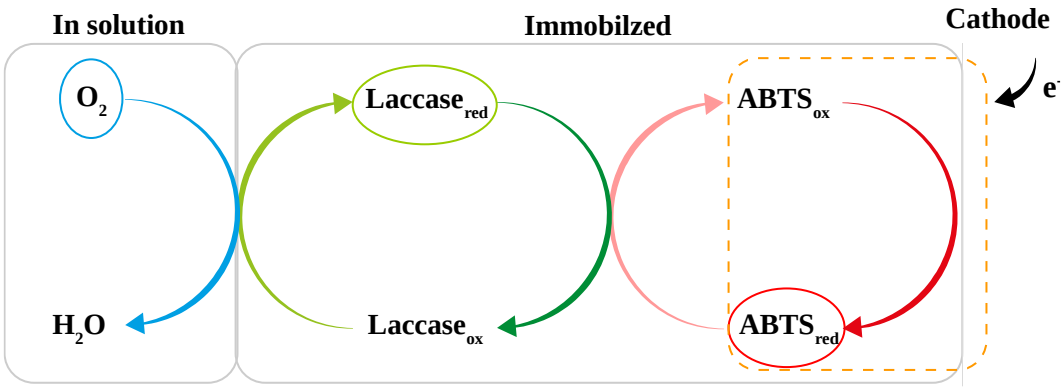

Figure 5. Schematic representation of the biocathode system

Fig. 6 shows the electrochemical response of the biocathode towards O_2electrocatalytic reduction in phosphate buffer solution pH 5 saturated with O_2. From the polarization curves, the oxygen reduction current begins at 0.6 V/ECS, with overpotential of 50 mV, and the current densities feature a semi-plateau that indicates the control of the electrocatalytic reaction by diffusion of the oxygen to the electrode surface. The biocathode based on Super P® (▲) shows improved kinetics of the electronic transfer and higher performance increase 500 µA cm^{-2} in 2-folds compared to biocathode based on KS6.

The first outcome to be observed from polarization curves is that the addition of carbon particles to the enzyme layers enhances bioelectrocatalytic processes. The large surface area of the particles enhances the reactive species loading and thus the available active sites for electron generation. Besides, the electronic conductivity of the carbon nanoparticles can enhance electron transfer rate to the electrodes. However, it is evident that bioelectrodes based on carbon Super P® display the best performances. The benefit of Super P® may be explained by its high porous structure that offers a close proximity to the reactive species and improves diffusion of oxygen within the enzyme films.

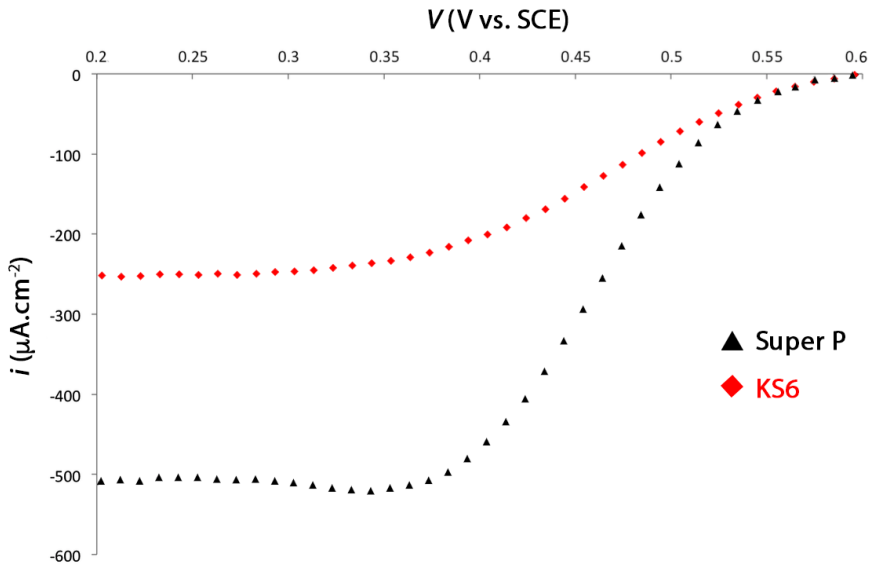

Figure 6. Polarization curve of an ABTS/laccase modified electrode in phosphate buffer solution (pH 5, 0.1 M) under O_2. Comparison between carbon powders KS6 and Super P®. Scan rate 3.33 mV s^{-1}.

The storage stability is reported in figure 7. On the opposite of the bioanode, biocathode shows a small decrease of activity and 20 % of initial current is still recorded after 28 days.

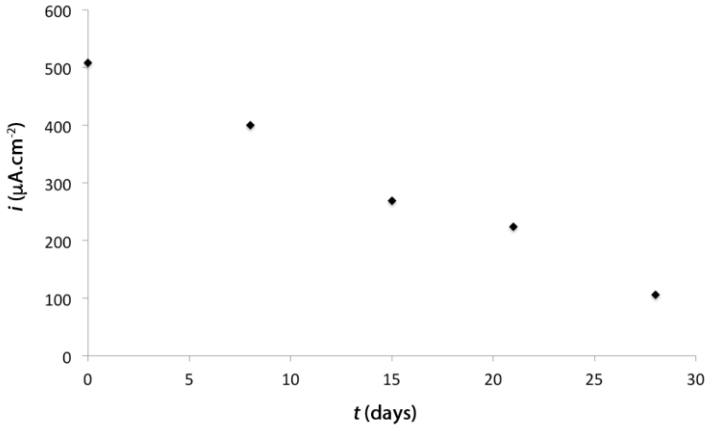

Figure 7. Biocathode stability, results based on polarization curves. Electrodes stored at 4°C under moist atmosphere after experiments.

This result demonstrates the good stability of the biocathode, probably due to the stability of laccase immobilized [25, 26] in our experimental conditions even if 20 % of initial value of current is recorded after 28 days [27]. A decrease of 50 to 60 % of the initial value has been already observed after 12 h [28]. Stability for a long time is a real limitation of this kind of system.

The operational stability has been studied by chronoamperometric curves characterization at 0.5 V/ECS. Figure 8 shows a current evolution with time. The initial value increases rapidly and reaches a stable value at 5000 s. This characterization confirms the stable response of the electrode in operating conditions.

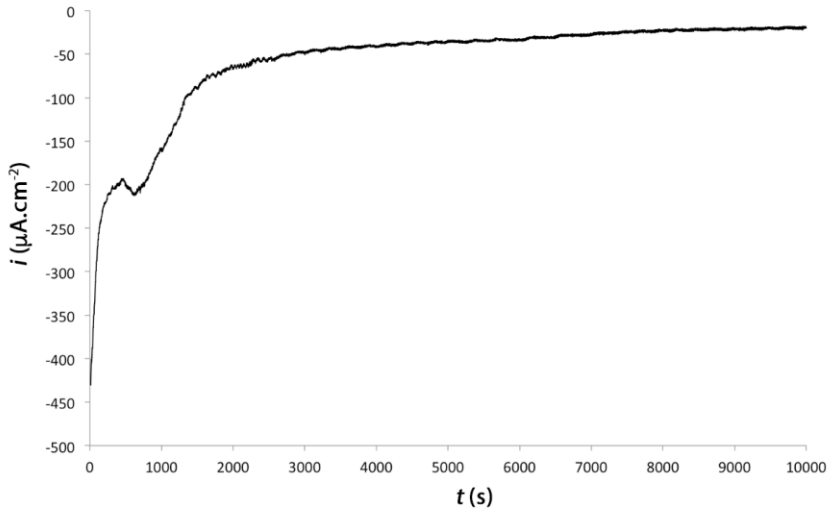

Figure 8. Chronoamperometric response at 0.5 V/SCE for a biocathode with carbon Super P® in phosphate buffer (pH 5, 0.1 M) under O_2.

3.4. Biofuel cell characterization

The good operational stability of bioanode based on carbon KS6 and biocathode based on carbon Super P allow application of these electrodes for biofuel cell construction.

The polarization curve and power output are depicted in figure 9.

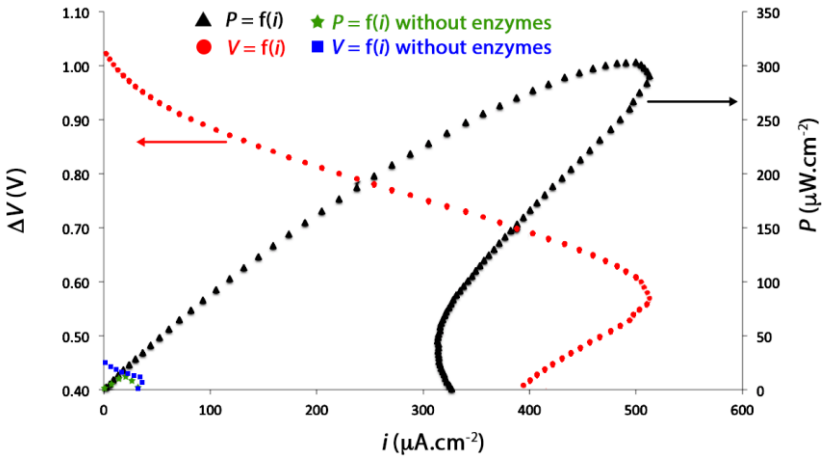

Figure 9. Polarization and power density curves of the biofuel cell using carbon KS6 at the anode and carbon Super P® at the cathode. Scan rate = 3.33 mV s^{-1}, with (black curve) and without enzymes (blue curve).

The initial open circuit potential of the biofuel cell was 1.02 V and the maximum power density was 300 $\mu W.cm^{-2}$. These results are in agreement with performances obtained with other ethanol biofuel cell [29, 30]. In our case, the open circuit potential value is higher than the value previously reported. The immobilization of mediator, specifically NAD^+, on the surface of electrode could explain this large open circuit potential. Indeed, all reacts are immobilized on the electrode and the potential is defined by amount of redox compound on the surface. A large amount of NAD^+ is located close to the enzyme and could react quickly without diffusion limitation.

The electrochemical characterization has been compared with power output given by connection of biofuel on the electrical resistance. In this last case, no potential and no current are applied on the electrodes. The values of potential and current are determined by the steady state of the both electrodes. An overshoot is observed in figure 9 corresponding to power density plot double back to the lower current after the maximum value is achieved. This kind of overshoot is frequently reported in the literature for the bioelectrochemical system based on the biological entities connected to the electrode [31]. It can be interpreted as the limitation of electrochemical circuit in presence of high current [32].

Figure 10 presents the evolution of current with time for two resistances: 400 and 40 000 Ω and electrical scheme used to connect the biofuel cell.

Surprisingly, the value of current with the larger resistance was highest. This result was thus not in accordance with the omic law which impose that when the resistance increases, the current decreases at constant potential.

This result suggests thus, that the value of potential can be affected by the current delivered by the biofuel cell. This point is clearly showed on figure 9, with polarization curve and power output. The both curves present a decrease of intensity for high values of potential and power.

On the polarization curve, the current decrease for a potential below to 0.55 V. The changing of shape of the curve can be explained by the modification of internal resistance. In other hand, if the resistance is maintained constant, modification of potential can be observed.

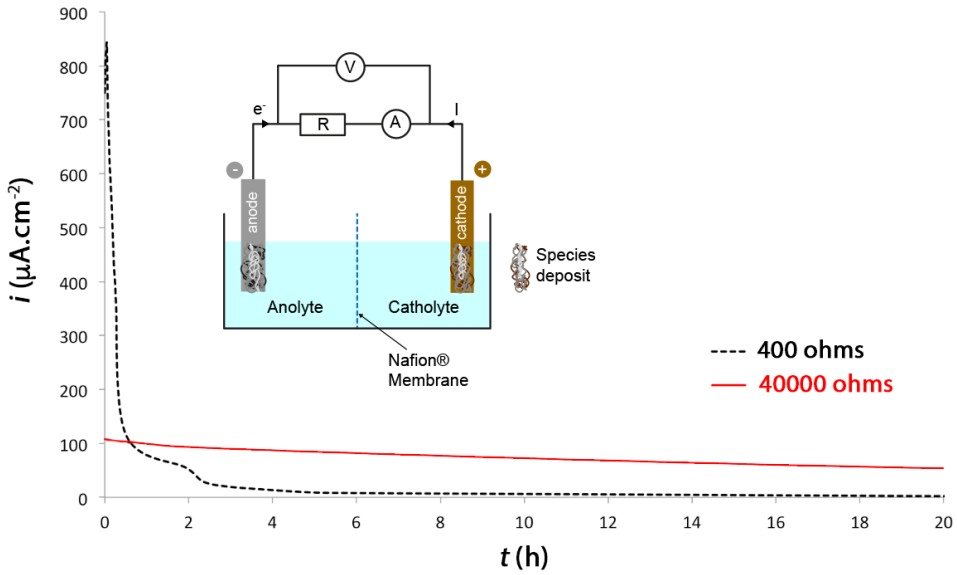

Figure 10. Evolution of the current density while the biofuel cell is connected to different resistances. Inset: Schematic representation of the biofuel cell with the resistance.

4. Conclusion

Enzymatic Biofuel cell for the generation of electrical energy from different organic substrates is promise to large development. The advantage of enzymatic catalyst is the number of substrate which can be used. In this study, we focused on the ethanol with NAD dependent enzyme as alcohol dehydrogenase,

We have shown the possibility to use an electrochemical multi enzymatic reaction for ethanol oxidation with simultaneous immobilization of enzyme and mediator on the surface of electrode modified with various carbon powders like KS6 and Super P carbon. Stability of the bioelectrode has been studied by electrochemical characterization. The effect of multi

enzymatic reaction has showed the importance of storage step. Chronoamperometric measurements demonstrated the efficiency of the ethanol enzymatic biofuel cell with immobilized mediators despite a weak performances recorded by polarization measurement. A high open circuit potential has been recorded (1,02 V), demonstrating the benefit of NAD^+ immobilization. Moreover, good performances have been recorded in terms of power density (300 $\mu W.cm^{-2}$). However, in the case of multi enzymatic reaction it is necessary to consider with great discernment the polarization measurement because of effect of potential applied on the enzymes. The current production with the high resistance gave good performances; 90 $\mu A.cm^{-2}$ during 20 hours.

References

1. Surendra KC, Khanal SK, Shrestha P, Lamsal B (2011) Current status of renewable energy in Nepal: Opportunities and challenges. Renew Sustain Energy Rev 15:4107–4117.
2. Escalona-Villalpando RA, Hasan K, Milton RD, et al (2019) Performance comparison of different configurations of Glucose/O2 microfluidic biofuel cell stack. J Power Sources 414:150–157.
3. Young TG, Hadjipetrou L, Lilly MD (1966) The theoretical aspects of biochemical fuel cells. Biotechnol Bioeng 8:581–593.
4. Yahiro AT, Lee SM, Kimble DO (1964) Biochimica et Biophysica Acta (BBA) - Specialized Section on Biophysical Subjects. Biochim Biophys Acta - Spec Sect Biophys Subj 88:375–383.
5. Kayali I, Qamhieh K, Fanun M, et al (2017) Transport properties of alternative fuel microemulsions based on sugar surfactant. J Dispers Sci Technol. 36:917–922.
6. Patrick JW (2004) Handbook of fuel cells. Fundamentals technology and applications. Fuel.
7. Bullen RA, Arnot TC, Lakeman JB, Walsh FC (2006) Biofuel cells and their development. Biosens. Bioelectron. 21: 2015–2045.

8. Kendall K (2002) Fuel cell technology: A sweeter fuel. Nat. Mater. 4: 211–2

9. Service RF (2002) Shrinking fuel cells promise power in your pocket. Science. 296:1222-1224.

10. Selloum D, Chaaya AA, Bechelany M, et al (2014) A highly efficient gold/electrospun PAN fiber material for improved laccase biocathodes for biofuel cell applications. J Mater Chem A 2:2794–2800.

11. Selloum D, Tingry S, Techer V, et al (2014) Optimized electrode arrangement and activation of bioelectrodes activity by carbon nanoparticles for efficient ethanol microfluidic biofuel cells. J Power Sources 269:834–840.

12. Ma S, Lu W, Mu J, et al (2008) Effect of immobilization supports on the amperometric response of silver nanoparticles enhanced glucose oxidase electrodes. J Dispers Sci Technol. 29:134–138.

13. Niiyama A, Murata K, Shigemori Y, et al (2019) High-performance enzymatic biofuel cell based on flexible carbon cloth modified with MgO-templated porous carbon. J Power Sources 427:49–55.

14. McCormick AJ, Bombelli P, Scott AM, et al (2011) Photosynthetic biofilms in pure culture harness solar energy in a mediatorless bio-photovoltaic cell (BPV) system. Energy Environ Sci. 4:4699–4709.

15. Veer Raghavulu S, Sarma PN, Venkata Mohan S (2011) Comparative bioelectrochemical analysis of Pseudomonas aeruginosa and Escherichia coli with anaerobic consortia as anodic biocatalyst for biofuel cell application. J Appl Microbiol. 110:666–674.

16. Karthikeyan R, Sathish Kumar K, Murugesan M, et al (2009) Bioelectrocatalysis of acetobacter aceti and Gluconobacter roseus for current generation. Environ Sci Technol. 22:8684–8689.

17. Reshetilov A, Alferov S, Tomashevskaya L, Ponamoreva O (2006) Testing of bacteria gluconobacter oxydans and electron transport mediators composition for application in biofuel cell. Electroanalysis.18:2030–2034.

18. Moore CM, Akers NL, Hill AD, et al (2004) Improving the environment for immobilized dehydrogenase enzymes by modifying nafion with tetraalkylammonium bromides. Biomacromolecules.5:1241–1247.

19. Antiochia R, Gallina A, Lavagnini I, Magno F (2002) Kinetic and thermodynamic aspects of NAD-related enzyme-linked mediated bioelectrocatalysis. Electroanalysis. 14:1256–1261.

20. Ogino Y, Takagi K, Kano K, Ikeda T (1995) Reactions between diaphorase and quinone compounds in bioelectrocatalytic redox reactions of NADH and NAD+. J Electroanal Chem. 396:517–524.

21 Zebda A, Tingry S, Innocent C, Cosnier S, Forano C, Mousty C (2011) Hybrid layered double hydroxides-polypyrrole composites for construction of glucose / O_2 biofuel cell. Electrochim Acta. 56:10378–10384.

22. Szabó T, Szeri A, Dékány I (2005) Composite graphitic nanolayers prepared by self-assembly between finely dispersed graphite oxide and a cationic polymer. Carbon N Y.43:87–94.

23. Wang Y, Alsmeyer DC, McCreery RL (1990) Raman Spectroscopy of Carbon Materials: Structural Basis of Observed Spectra. Chem Mater. 5:557–563.

24. Sakai H, Nakagawa T, Mita H, et al (2009) A high-power glucose/oxygen biofuel cell operating under quiescent conditions. Energy Environ Sci. 2:133–138.

25. Brunel L, Denele J, Servat K, et al (2007) Oxygen transport through laccase biocathodes for a membrane-less glucose/O_2 biofuel cell. Electrochem commun. 9:331–336.

26. Merle G, Habrioux A, Servat K, et al (2009) Long-term activity of covalent grafted biocatalysts during intermittent use of a glucose/O_2 biofuel cell. Electrochim Acta. 54:2998–3003.

27. Manoand N, Poulpiquet N (2018) O_2 Reduction in Enzymatic Biofuel Cells. Chem. Rev. 118:2392−2468.

28. Franco J H, Minteer S D, Andrade A R (2018) Product Analysis of Operating an Ethanol/O_2 Biofuel Cell Shows the Synergy between Enzymes within an Enzymatic Cascade. Journal of The Electrochemical Society. 9:H575–H579

29. Topcagic S, Minteer SD (2006) Development of a membraneless ethanol/oxygen biofuel cell. In: Electrochimica Acta. 51:2168–2172.

30. Deng L, Shang L, Wen D, et al (2010) A membraneless biofuel cell powered by ethanol and alcoholic beverage. Biosens Bioelectron. 26:70–73.

31. Angioni S, Millia L, Bruni G, Ravelli D, Mustarelli P, Quartarone E (2017) Novel composite polybenzimidazole-based proton exchange membranes as efficient and sustainable separators for microbial fuel cells, J. Power Sources. 348:57–65.

32. Pasternak G, Greenmann J, Ieropoulos I (2016) Comprehensive Study on Ceramic Membranes for Low- Cost. Microbial Fuel Cells. ChemSusChem. 9:88–96.